Radiation and Environmental Biophysics
https://doi.org/10.1007/s00411-019-00800-6

ORIGINAL ARTICLE

Exposure–lag–response associations between lung cancer mortality and radon exposure in German uranium miners

Matthias Aßenmacher[1] · Jan Christian Kaiser[2] · Ignacio Zaballa[3] · Antonio Gasparrini[4,5,6] · Helmut Küchenhoff[1]

Received: 6 December 2017 / Accepted: 5 June 2019

Abstract

Exposure–lag–response associations shed light on the duration of pathogenesis for radiation-induced diseases. To investigate such relations for lung cancer mortality in the German uranium miners of the Wismut company, we apply distributed lag non-linear models (DLNMs) which offer a flexible description of the lagged risk response to protracted radon exposure. Exposure–lag functions are implemented with B-Splines in Cox models of proportional hazards. The DLNM approach yielded good agreement of exposure–lag–response surfaces for the German cohort and for the previously studied cohort of American Colorado miners. For both cohorts, a minimum lag of about 2 year for the onset of risk after first exposure explained the data well, but possibly with large uncertainty. Risk estimates from DLNMs were directly compared with estimates from both standard radio-epidemiological models and biologically based mechanistic models. For age > 45 year, all models predict decreasing estimates of the Excess Relative Risk (ERR). However, at younger age, marked differences appear as DLNMs exhibit ERR peaks, which are not detected by the other models. After comparing exposure–responses for biological processes in mechanistic risk models with exposure–responses for hazard ratios in DLNMs, we propose a typical period of 15 year for radon-related lung carcinogenesis. The period covers the onset of radiation-induced inflammation of lung tissue until cancer death. The DLNM framework provides a view on age-risk patterns supplemental to the standard radio-epidemiological approach and to biologically based modeling.

Keywords Uranium miners · Radon exposure · Lung cancer mortality · Distributed lag non-linear models · Exposure–lag–response surface

Introduction

Lung cancer is the most frequent cause of death among all cancer diseases (Fitzmaurice et al. 2017). The predominant risk factor is tobacco smoke followed by anthropogenic environmental radiation exposure, but a good understanding of the biological processes leading to lung cancer is still lacking (Alberg et al. 2013). Epidemiological risk assessment provides a powerful tool to establish statistical associations between exposure to ionizing radiation and late health effects. Radio-epidemiological models rely on a comprehensive description of the radiation risk with appropriate mathematical functions. In their standard form, they apply a response function to the total radiation exposure, which is modified by various predictor variables, often called effect modifiers (EMs). For acute exposure, these variables include sex, age at exposure, and attained age. Risk assessment for protracted exposure requires a detailed exposure history, which has been estimated for several carcinogenic

✉ Matthias Aßenmacher
matthias.assenmacher@stat.uni-muenchen.de

1 Department of Statistics, Ludwig-Maximilians-Universität, 80539 Munich, Germany

2 Institute of Radiation Medicine, Helmholtz Zentrum München, 85764 Oberschleißheim, Germany

3 Miramar Kalea 11-2, Getxo 48992, Spain

4 Department of Social and Environmental Health Research, London School of Hygiene and Tropical Medicine, 15–17 Tavistock Place, London WC1H 9SH, UK

5 Department of Medical Statistics, London School of Hygiene and Tropical Medicine, Keppel Street, London WC1E 7HT, UK

6 Centre for Statistical Methodology, London School of Hygiene and Tropical Medicine, Keppel Street, London WC1E 7HT, UK

Published online: 19 June 2019

agents in the German uranium miners cohort of the Wismut company for the period 1946–1989. Smoking information is only available for part of the cohort (Kreuzer et al. 2018). However, for exposure to radon and its short-lived progeny, which constitutes the second most important lung carcinogen, annual exposures were estimated for each miner from begin to end of employment. Thereafter, cohort members were subjected to a mortality follow-up until 2003 as end of follow-up for the present study (Kreuzer et al. 2010). Overall, the mortality follow-up has been executed until 2013. Lung cancer risks have been studied extensively in the Wismut cohort with complex radio-epidemiological models (Kreuzer et al. 2015; Walsh et al. 2010, 2010). Studies on all late health effects are reviewed by Walsh et al. (2015).

Applying the total exposure–response with EM adjustment for risk estimation represents the quasi-standard approach in radiation epidemiology. It is generally accepted by committees BEIR VI (1999), NRC (2006), UNSCEAR (2009), and ICRP (Valentin 2007) which issue recommendations for radiation protection. On the other hand, this descriptive approach provides little insight into cancer etiology. To make progress here, the present study investigates the distribution of time lags between exposure and outcome. It reflects the duration of disease development, thereby supporting a biologically based analysis of observational cancer data. Until now, only a few radio-epidemiological studies have addressed this aspect.

In the cohort of Japanese a-bomb survivors, the radiation risk arises from a single event of acute exposure. For leukemia, mortality of a-bomb survivors (Richardson et al. 2009) has reported a peak in the Excess Relative Risk (ERR) 10 year after exposure. A lognormal lag function with only two parameters provided a good description of the data. For protracted exposure, a lagged response cannot be gleaned directly from incidence, data but can be uncovered by disentanglement of the exposure–lag–response. Several approaches have been tested on the cohort of Colorado Plateau uranium miners, which exhibits exposure patterns similar to the Wismut cohort but with additional records for smoking habits (Schubauer-Berigan et al. 2009). Pertinent studies are built on the assumption that exposure in short constant age intervals contributes additively to the radiation risk albeit with differential weight (Berhane et al. 2008; Gasparrini 2014; Hauptmann et al. 2001).

Hauptmann et al. (2001) analyzed exposure–lag relationships using spline weight functions. Deviating from the standard radio-epidemiological approach as described above, they applied a linear risk response to the *exposure rate*.[1] Armstrong (2006) and Berhane et al. (2008) extended this scheme to accommodate time-varying exposure.

Gasparrini (2011, 2014) applied a more general framework for the analysis of exposure–lag–response associations in the cohort of Colorado Plateau uranium miners using *distributed lag non-linear models* (DLNMs). Such models are constructed by a flexible bivariate *exposure–lag–response surface*, which maintains the linearity of model parameters. Consistent with the previous studies, (Berhane et al. 2008; Hauptmann et al. 2001; Gasparrini 2014) estimated a similar shape for the lag–response curve, which was constructed with quadratic B-splines.

Implemented as a package in R (R Core Team 2019), the DLNM framework offers convenient versatility to describe model non-linearities and distributed lag effects (Gasparrini 2011). It features an algebraic definition of standard errors, confidence intervals, and tests; allows for a flexible use of different functions for each dimension; and provides a well-designed tool for interpreting results.

Zaballa and Eidemüller (2016) applied a biologically based Two-Stage Clonal Expansion (TSCE) model to the Wismut cohort. Their mechanistic analysis was concerned with biological aspects of lung carcinogenesis such as oncogenic mutations and the growth dynamics of pre-cancerous lesions. As biological target of radon exposure, they proposed clonal expansion of initiated cells increased by radiation-induced inflammation. The mechanistic TSCE model is fully capable of providing risk estimates for comparison with standard risk models. Thus, to put the results of the TSCE model into perspective, they applied a modified version of the preferred ERR model from Walsh et al. (2010) as reference.

In the cohort of Colorado miners, about 260 lung cancers cases have been recorded until end of 1982, compared to about 3000 cases in the Wismut cohort followed up until 2003. As the largest cohort of uranium miners in the world to date, the Wismut cohort offers a unique opportunity to validate the results of Gasparrini (2014) for the Colorado Plateau uranium miners. With the present study, we examine response functions of the hazard ratio related to both annual radon exposure and time since exposure. Second, estimates of the ERR from our preferred DLNM are compared with results from both mechanistic models and standard radio-epidemiological models applied in the study of Zaballa and Eidemüller (2016). Our main interest here is to assess the ability of risk models to represent plausible exposure–lag–response associations. Finally, by comparing results from DLNMs and biologically

[1] In the standard radio-epidemiological approach, exposure–response is related to cumulative exposure, whereas exposure–response in the DLNM framework is related to *exposure rate*.

based risk models, we speculate on the duration of development for radon-related lung cancer.

Materials and methods

The Wismut cohort

In March 2016, we obtained access to the Wismut cohort data set from the German Federal Office for Radiation Protection (Bundesamt für Strahlenschutz (BfS)) by transfer agreement. The full data set comprises 58,987 men who were formerly employed at the Wismut company in the years from 1946 to 1989. Radiation exposure was estimated using a detailed job-exposure matrix (JEM), which includes information on exposure to radon and its progeny in WLM, external radiation in units of mSv and long-lived radionuclides (^{235}U, ^{238}U) in units of kBq h/m^3. The JEM provides exposure values for each calendar year of employment between 1946 and 1989, each place of work and each type of job. More than 900 different jobs and 500 different working places were evaluated for this purpose. Radon (^{222}Rn) measurements in the Wismut mines were carried out from 1955 onwards. For the period from 1946 to 1954, radon concentrations were estimated retrospectively by an expert group based on measurements from 1955, taking into account specific mining conditions in the early period. From 1955 to 1965, about 57,000 radon gas measurements were taken in Saxonian underground mines, from 1966 to 1990, about 140,000 radon progeny measurements were performed. The corresponding numbers for Thuringian underground mines are about 39,000 radon measurements between 1955 and 1974, and about 160,000 radon progeny measurements from 1975 to 1990. For each calendar year and each mining object, individual exposure estimates were assigned to all cohort members. More details on exposure estimation and uncertainty assessment are given in the reports of Lehmann et al. (1998) and Lehmann (2004) and of Küchenhoff et al. (2018).

Due to missing values for silica dust exposure, 292 members were excluded, so that 58,695 workers contributed to the present analysis. A miner was considered at risk from date of first employment until date of death, date of loss to follow-up or end of follow-up (December 31, 2003). In total, 20,757 deaths occurred as 35.4% of the full cohort of which 2,996 deaths (5.1%) were attributed to lung cancer. For a more circumstantial description of the Wismut cohort, see ref. (Kreuzer et al. 2010).

The Cox model

Theory

For risk assessment, we apply an extension of Cox's model of proportional hazards to allow for non-linearity and lagged effects in exposure-related covariables using the algebraic notation:

$$\lambda(t,x,z,cal,abe) = \lambda_0(t)\cdot\exp\left[s_x(x,t) + s_z(z,t) + \gamma\, cal + \delta\, abe\right], \tag{1}$$

with s_x (radon) and s_z (silica dust) as non-linear exposure covariables, calendar time *cal* (centered around the year 1970), and the age at begin of employment *abe* as linear covariables.

Inference

Inference in the Cox model is performed via the partial likelihood approach, using Efron's method (Efron 1977) for tie handling, which allows to skip the estimation of the nuisance parameter $\lambda_0(t)$ to reduce complexity (Cox 1975). Risk estimates are expressed as hazard ratios (HRs). The statistical analysis was performed using the packages `survival` (Therneau 2015; Therneau and Grambsch 2000) and `dlnm` (Gasparrini 2011) within the statistical software `R` (R Core Team 2019; RStudio Team 2015). The figures were created using the package `ggplot2` (Wickham 2016).

The DLNM framework

As the analysis is based on an approach introduced by Gasparrini and colleagues (Gasparrini 2014; Gasparrini et al. 2010, 2017), we will give a brief summary of the mathematical background and the inference methods. While Gasparrini et al. (2010) are mainly concerned with time series analysis, Gasparrini (2014) applies the methodology to analyze time-to-event data with the Cox model. Gasparrini et al. (2017) focus on the extension to a penalized framework. Bender et al. (2018) use a piecewise exponential model for a flexible analysis of lagged effects. We start with an introduction of the simpler distributed lag models (DLMs), which are then extended to accommodate more complex non-linearities (Gasparrini 2014).

Distributed lag models (DLMs)

DLMs describe the lag–response relationship for a linear effect of exposure, understood here as annual rates for exposure to radon and its short-lived progeny. Gasparrini (2014) describes the relation in the following form:

$$s(x,t) = \int_{\ell_0}^{L} x_{t-\ell}\cdot w(\ell)\, d\ell \tag{2a}$$

$$\approx \sum_{\ell=\ell_0}^{L} x_{t-\ell}\cdot w(\ell), \tag{2b}$$

where $w(\ell)$ is the so-called lag–response function.

In Eq. (2a), $L - \ell_0$ defines the period, while exposure has an effect on outcome. Equation (2b) is an approximation of the integral (2a). An optimal value for the minimum lag ℓ_0 will be searched in the present study. The maximum lag L is confined to 40 year after exposure as in ref. (Gasparrini 2014), although some cohort members are followed up for 57 years.

Expressing $s(x, t)$ in matrix notation yields the following:

$$s(x,t;\boldsymbol{\eta}) = \mathbf{q}_{i,t}^{\top}\,\mathbf{C}\boldsymbol{\eta} = \mathbf{w}_{i,t}^{\top}\,\boldsymbol{\eta}, \tag{3}$$

where $\mathbf{q}_{i,t} = (x_{i,t-\ell_0}, \ldots, x_{i,t-\ell}, \ldots, x_{i,t-L})^{\top}$ and $\mathbf{C}$ as a transformation of the lag vector ℓ with a vector of dimension $v_{\ell}^{\top}$ defining the basis functions. Therefore, Eq. (3) is the vectorial representation of Eq. (2a) with adjustable parameters $\boldsymbol{\eta}$ as coefficients for B-Splines.

Distributed lag non-linear models (DLNMs)

Allowing for non-linearity in x and giving up the assumption of independence of $f(.)$ and $w(.)$ yield the following:

$$s(x,t) = \int_{\ell_0}^{L} f \cdot w(x_{t-\ell}, \ell)\, d\ell \tag{4a}$$

$$\approx \sum_{\ell=\ell_0}^{L} f \cdot w(x_{t-\ell}, \ell), \tag{4b}$$

where $f \cdot w(x_{t-\ell}, \ell)$ is a truly bivariate function in x and in t. This constitutes an *exposure–lag–response surface* (Gasparrini 2014), which is parameterized with a special tensor product, called *cross-basis* (Armstrong 2006).

By defining[2] the following:

$$\mathbf{A}_{i,t} = \left(\mathbf{R}_{i,t} \otimes \mathbf{1}_{v_{\ell}}^{\top}\right) \odot \left(\mathbf{1}_{v_x}^{\top} \otimes \mathbf{C}\right), \tag{5}$$

the cross-basis function can be written as follows:

$$s(x,t;\boldsymbol{\eta}) = \left(\mathbf{1}_{L-\ell_0+1}^{\top}\mathbf{A}_{i,t}\right)\boldsymbol{\eta} = \mathbf{w}_{i,t}^{\top}\,\boldsymbol{\eta}_x. \tag{6}$$

Similar to $\mathbf{C}$ in Eq. (3), $\boldsymbol{R}_{i,t}$ is constructed by transforming $\mathbf{q}_{i,t}$ with a vector of dimension v_x. The identifiabilty issues mentioned by Gasparrini (2014) do not apply here as we do not include intercepts in the basis functions for exposure covariables x and z in $s_x(x, t)$ and $s_z(z, t)$, respectively.

[2] $\otimes$ denotes the Kronecker product, while $\odot$ denotes the Hadamard product

Model selection

Model selection is performed with goodness-of-fit measured by the Akaike information criterion (AIC) and the Bayesian information criterion (BIC). These two criteria are given as follows:

$$\mathrm{AIC} = -2 \cdot \mathcal{L}(\hat{\boldsymbol{\eta}}_x, \hat{\boldsymbol{\eta}}_z, \hat{\gamma}, \hat{\delta}) + 2 \cdot df \tag{7a}$$

$$\mathrm{BIC} = -2 \cdot \mathcal{L}(\hat{\boldsymbol{\eta}}_x, \hat{\boldsymbol{\eta}}_z, \hat{\gamma}, \hat{\delta}) + \ln(n) \cdot df, \tag{7b}$$

where n is the number of uncensored events (i.e., lung cancer deaths) and df is the degree of freedom (or model parameters). Parameters estimates are calculated for B-spline coefficients in the exposure–lag–response relations for radon $\hat{\boldsymbol{\eta}}_x$ and silica dust $\hat{\boldsymbol{\eta}}_z$, and for adjustment to calendar year $\hat{\gamma}$ and age at begin of exposure $\hat{\delta}$.

In the primary analysis to this study [Master thesis of Aßenmacher (2016)], some 50 models have been fitted. We chose model selection by AIC as the method of choice, although slight over-fitting can come with it. On the other hand, BIC selection produced too sparse models, which tend to overlook important features of the data. In addition, we report results of LRTs, to support the findings obtained by comparison of AIC vs. BIC where possible.

To avoid biologically implausible exposure–lag–response surfaces, we applied an additional *criterion of wiggliness*. In the lag–response relationship, curves with *wiggly* courses are not accepted. Wiggly curves are defined as *having more than one change in slope from positive to negative or vice versa*. The criterion is motivated by the assumption that protracted exposure of limited duration causes health effects, which peak after a typical time since exposure and decline thereafter.

Descriptive ERR model of Zaballa and Eidemüller

For comparison with the results of our study, we apply the descriptive ERR model of Zaballa and Eidemüller (2016)

$$\begin{aligned}\mathrm{ERR}_{\,r} =& \beta_r\, D\left[1 + \alpha_{t1}(t_{\mathrm{sme}} - 11) + \alpha_{t2}(t_{\mathrm{sme}} - 11)^2\right] \\ & \cdot \exp\left[-\alpha_a(a - 44) - \alpha_r(d_{\mathrm{avg}} - 32.4)\right]\end{aligned} \tag{8}$$

with central ERR coefficient β_r for cumulative radon exposure and EMs for time since median exposure t_{sme}, attained age a, and mean exposure rate d_{avg} expressed in working level months per year (WLM/yr). Maximum-likelihood estimates for model parameters are given in Table 4 of Zaballa and Eidemüller (2016). Note that, for their biologically based TSCE model, no closed analytical form can be given.

Table 1 Properties and goodness-of-fit for DLNMs NL1 to NL4 with exposure-(rate)-response $f(x_{t-\ell})$ constructed from B-splines of degree 2 with 2 knots at 1.6 WLM/yr and 16.5 WLM/yr; for the lag–response $w_x(\ell)$, the knot is placed at 20 year, *df* denotes the number of model parameters, and lowest values for AIC and BIC in bold

Model	$w_x(\ell)$	AIC	BIC	*df*
NL1	Constant	58241.75	**58295.79**	9
NL2	B-Spline (degree 2, 1 knot, intercept)	58234.52	58360.62	21
NL3	B-Spline (degree 2, 1 knot, right-constrained)	58295.72	58349.77	9
NL4	B-Spline (degree 2, 1 knot)	**58232.44**	58334.52	17

We also carried out LRTs where NL2 was tested against NL1 ($p < 0.01$) and NL4 ($p = 0.205$). The tests indicate a superior goodness-of-fit of NL2 compared to NL1, but no superiority compared to NL4 (despite the inclusion of the intercept). NL4 is our preferred model

Results

We systematically explored a large number of models to determine our preferred DLNM. The model design is successively revised by variation of the cross-basis in Eq. (6). Each model is assessed by its goodness-of-fit and biological plausibility. Suitable adjustments for silica dust and minimum lag ℓ_0 for radon exposure have been examined with simpler DLMs. To limit the number of test calculations, these adjustments have been retained for the more complex DLNMs without modification. Results of our investigations are summarized here; more detailed information is given in the "Appendix" section and in the primary analysis (Aßenmacher 2016).

DLMs

DLMs rely on a linear relationship of the response to the annual radon exposure rate $x_{t-\ell}$ given in Eq. (2b). For the lag–response function $w_x(\ell)$, various forms have been tested as reported in ''Appendix'' section. At the onset, the HR dependence on exposure to silica dust has been determined. The exposure–response function $f(z_{t-\ell})$ for silica dust is specified as a linear threshold function, and the lag–response function $w_z(\ell)$ is chosen as piecewise constant with two cut-off points. The minimum lag ℓ_0 was set to 2 year. The lag–response association of our preferred DLM L5 is shown in Fig. 7. Table 2 summarizes properties and goodness-of-fit (including p values of LRTs) for a selected number of DLMs.

DLNMs

The evaluation of DLMs already showed that B-splines of higher degrees are not suited for modeling the lag–response. Consequently, B-splines of degrees five and six are no longer considered (Aßenmacher 2016). B-splines of degree one are discarded a-priori as they possibly oversimplify the true underlying relationship. Concerning the knots and their placement, up to five knots on equally spaced quantiles of the lag distribution were chosen.

For the characterization of the exposure–response function, B-splines are applied, as well. In this case, B-splines of degree two, three, and four in combination with 0–5 knots at equally spaced quantiles of the exposure distribution are taken into consideration. The AIC-selected models characterize the exposure–response well. The 20 AIC-best models all include a B-Spline of degree two with two knots at 33.3% and the 66.6% quantiles of the exposure distribution. Within these models, considerable variation was observed for the lag–response, but none of the AIC-best models contains a B-Spline with more than three knots. Table 1 summarizes the properties and goodness-of-fit for selected DLNMs, which all apply the same B-splines of degree two for the preferred non-linear risk response to annual radon exposure. Compared to the preferred DLM L5, nearly all models improve the AIC by about hundred points.

Minimum lag period

In the primary analysis to this study, special attention has been given to the characterization of the minimum lag period for risk onset (Aßenmacher 2016). Minimum lag ℓ_0 was defined as the time after (first) exposure when the HR exceeds a biologically plausible threshold of one. Using a heuristic method, some 50 models have been examined with a minimum lag varying between 0 and 5 year. Based on goodness-of-fit, models with a minimum lag between 2 and 3 yr yielded a good data description. Models with longer minimum lag provided markedly inferior fits.

We reexamined the estimation of ℓ_0 by considering model NL2 which allowed for flexible minimum lags depending on exposure rate, as shown in Fig. 1. In model NL2, the intercept varies weakly with exposure rate and is compatible with a 2 year minimum lag. Model NL4 with a fixed minimum lag at 2 year yields a slightly lower AIC than model NL2, but, with four intercept-related parameters less, its BIC is considerably lower (Table 1).

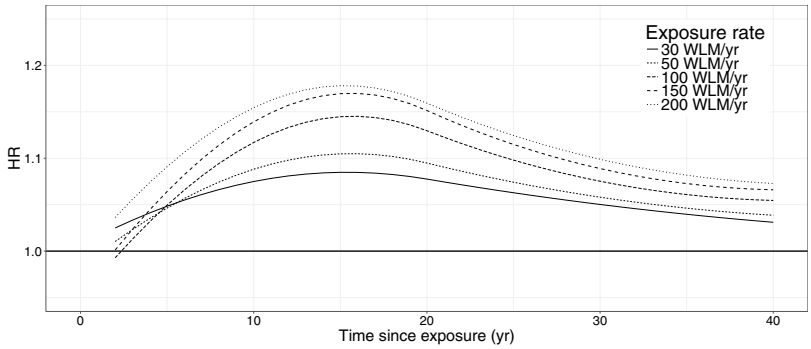

Fig. 1 Lag–response curves for the hazard ratio (HR) of model NL2 for exposure rates of 30–200 WLM/yr; model NL2 was used to estimate minimum lags

Behavior long after exposure

To investigate the behavior long after exposure, the lag–response function in DLNM NL3 was right-constrained to HR = 1 at time since exposure 40 year. Compared to models NL4 and NL2 without right constraint, the information criteria AIC and BIC were markedly increased, suggesting a significant residual lung cancer risk more than 40 yeary after exposure (Table 1). Figures 8 and 9 in "Appendix" section depict lag–response curves, exposure–response curves, and the complete exposure–lag–response surface of model NL3.

Preferred DLNM

After assessing DLNMs NL1–NL4 based on goodness-of fit and biological plausibility, we choose NL4 as our preferred DLNM. Model NL4 satisfies the criterion of wiggliness and has an AIC of about 113 points lower than the preferred DLM L5 (Table 1, Fig. 7 in "Appendix" section). It contains a cross-basis with a B-spline of degree two with two knots for the exposure–response function at 1.6 WLM/yr and 16.5 WLM/yr, and a B-spline of degree two with one knot at a lag of 20 years for the lag–response. Estimates for the cross-basis coefficients are given in Table 4 in "Appendix" section.

Age-risk patterns of the preferred DLNM

The exposure–lag–response surface is shown in Fig. 2 and selected lag–response curves and exposure–response curves are depicted in the upper panels of Fig. 3. Peak hazard ratios appear about 15 year after exposure to any annual radon exposure rate from 5 to 300 WLM/yr. The lag–response flattens for time since exposure > 30 year, but does not vanish at the end of the lag period $L = 40$ year.

The exposure–response increases sharply below an exposure rate of about 20 WLM/yr and then reverts to a smaller slope until about 200 WLM/yr. For exposure > 200 WLM/yr, a small drop in the exposure–response is observed for time since exposure < 30 year. However, for larger lag times, the increase continues. At very low exposure rates, < 5 WLM/yr hazard ratios become smaller than one. Such protective effects at low exposure rates have been reported for animal experiments (Heidenreich et al. 1999). However, they are not in the focus of the present study and may well be attributed to mathematical artifacts of knot placement. Estimates for confounders age at begin of employment, calendar year, and silica dust exposure for the preferred DLNM NL4 are given in Table 3 and Fig. 10 in "Appendix" section.

Baseline rates from the preferred DLNM NL4 are displayed in Fig. 11 of "Appendix" section for age intervals of 5 years and six calendar year periods between 1946 and 2003. Baseline rates from both the mechanistic and the descriptive models exhibit an attenuation or even a decrease at old age (results not shown). Compared to baseline rates from the preferred DLNM NL4, they possibly provide a more

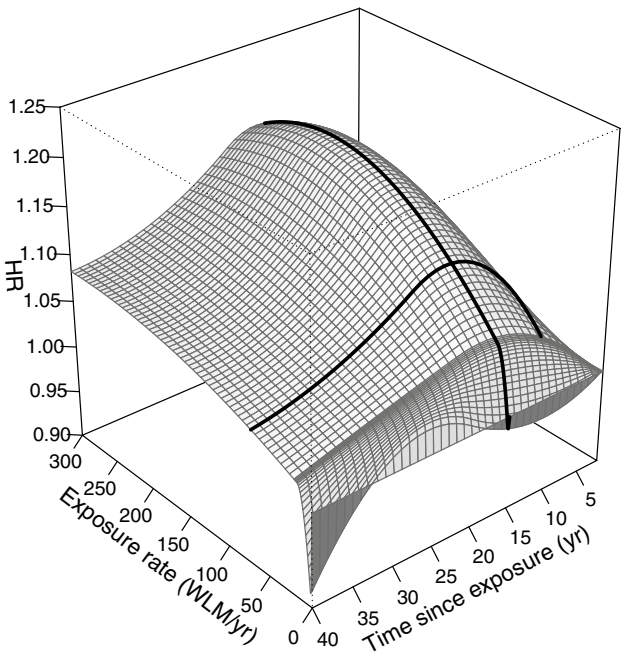

Fig. 2 Exposure–lag–response surface for the hazard ratio (HR) of the preferred DLNM NL4, two solid lines along the surface delineate a lag–response curve at exposure 70 WLM/yr, and an exposure–response curve at time since exposure 15 year, and at exposure rates < 5 WLM/yr, the HR becomes < 1

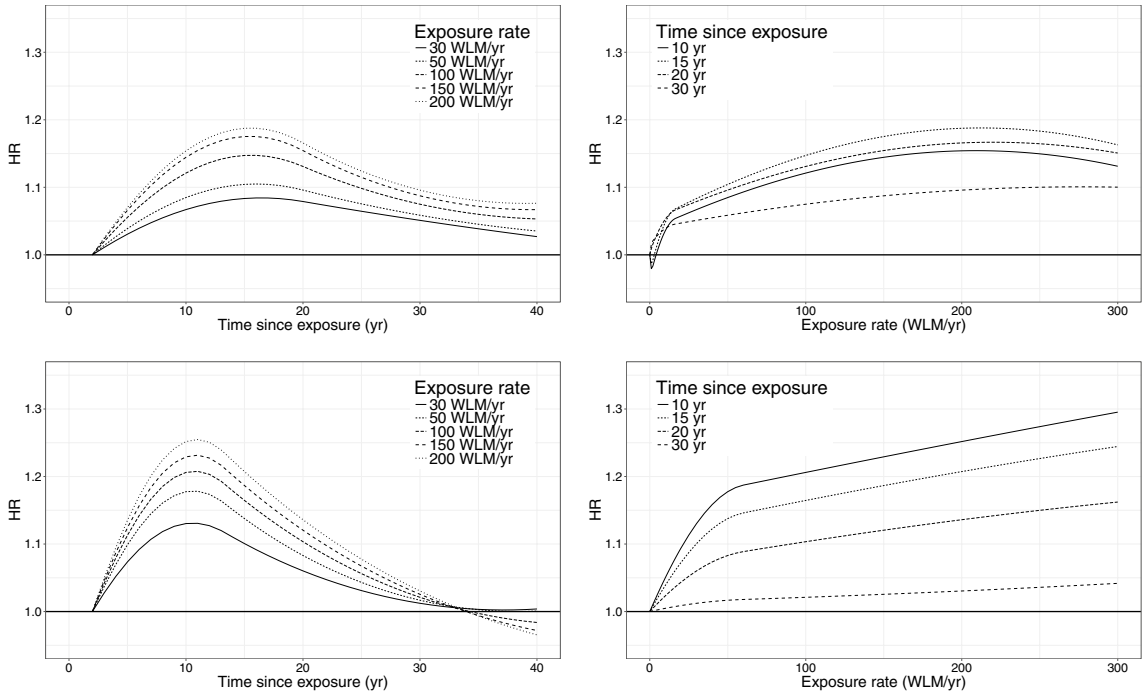

Fig. 3 Selected lag–response curves of the hazard ratio (HR) for radon exposure rates between 30 and 200 WLM/yr (left panels) and exposure–response curves of the HR for time since exposure between 10 and 30 year (right panels) for our preferred DLNM NL4 (top panels) to model 8 by Gasparrini (2014) (bottom panels)

accurate description of the male lung cancer mortality in Germany, but a deeper investigation of baseline rates is beyond the scope of the present study.

Exposure scenarios

To compare risk estimates of our preferred DLNM NL4 with those of the standard radio-epidemiological ERR model (cited in Eq. 8) and the biologically based TSCE model, both from Zaballa and Eidemüller (2016), we consider scenarios motivated by the distribution of covariables age of death, age at median exposure, exposure duration, exposure rate, and cumulative lifetime exposure, as summarized in Table 5. Birth year 1930 was assumed for a miner without silica exposure and the period of exposure was centered around median age 26 year in 1956. For the scenario calculations, 12.5 WLM/yr was chosen as minimal exposure rate, although mean exposure rates of 7 WLM/yr for miners employed after 1955 and 1.4 WLM/yr for miners employed after 1959 were markedly lower. However, for such low exposure rates, the exposure–response of the preferred DLNM NL4 is burdened with considerable uncertainty and should not be applied (Figs. 2, 3).

For a scenario of constant cumulative exposure 100 WLM and 400 WLM with duration of 4 year and 8 year lung cancer, mortality was considered for attained age from 40 to 80 year, corresponding to calendar years 1970–2010. Figure 4 depicts estimates for the age dependence of the ERR. Due to the DLNM construction for Cox regression in Eq. 1, the corresponding $\mathrm{ERR} = \lambda(x = d)/\lambda(x = 0) - 1 = \exp[s_x(x = d, t)] - 1$ depends only on exposure rate d and time since exposure t, whereas dependencies on calendar year *cal* and age at begin of employment *abe* cancel out.

For a scenario of constant exposure rates 12.5 WLM/yr and 100 WLM/yr, Fig. 5 shows estimates of the ERR for attained age 60 year in 1990 depending on radon exposure accumulated by increasing exposure duration up to 12 year. Risk dependence on cumulative exposure is considered here to assess the range of applicability for the linear no-threshold (LNT) paradigm in radiation protection.

Discussion

Comparison with the preferred DLNM for the Colorado cohort

Figure 3 compares lag–response and exposure–response curves from our preferred DLNM NL4 with those from the preferred DLNM model 8 for the Colorado cohort (Gasparrini 2014). Exposure–lag–response relationships from both studies produced similar estimates for hazard ratios in the range between 1.2 and 1.3. Despite missing adjustment

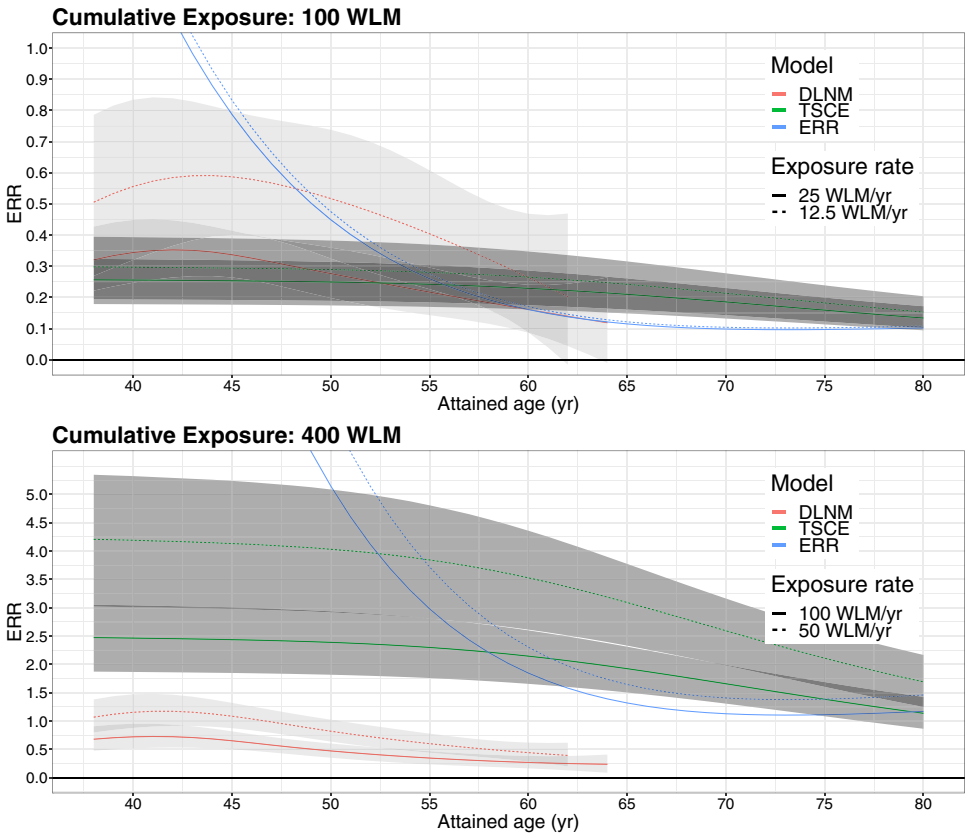

Fig. 4 Estimates of the ERR depending on attained age for cumulative exposure to 100 WLM at exposure rates 12.5 WLM/yr and 25 WLM/yr (upper panel) and for cumulative exposure to 400 WLM at exposure rates 50 WLM/yr and 100 WLM/yr (lower panel) at age of median exposure 26 year for the preferred DLNM (red), the TSCE model (green) and the ERR model (blue), and shaded areas display 95% CIs of the preferred DLNM (light gray) and the TSCE model (dark gray) (color figure online)

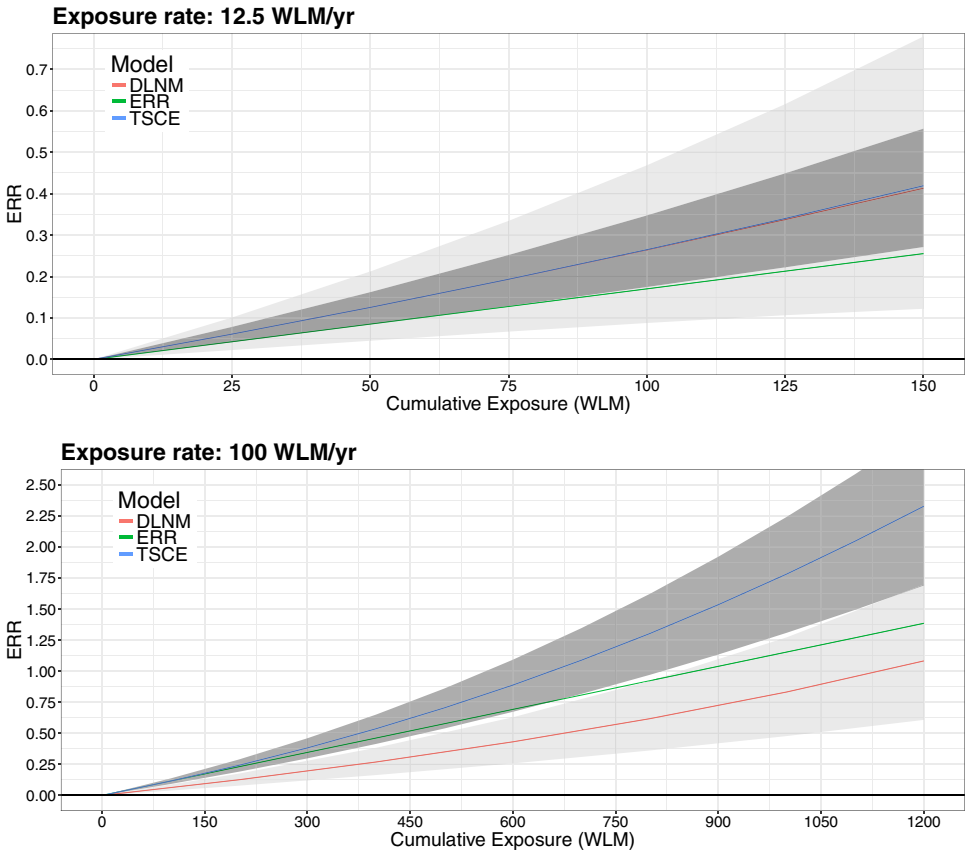

Fig. 5 Estimates of the ERR depending on cumulative radon exposure for the preferred DLNM (red), the TSCE model (blue), and the ERR model (green) for scenarios with age at median exposure 26 year, attained age 60 year, and constant exposure rates 12.5 WLM/yr (upper panel), 100 WLM/yr (lower panel) for exposure duration up to 12 year, and shaded areas display 95% CIs of the preferred DLNM (light gray) and the TSCE model (dark gray), for the lower exposure rate 12.5 WLM/yr DLNM and TSCE model give the same result (color figure online)

for smoking in the Wismut cohort and missing adjustment for silica dust in the Colorado cohort, estimates from both cohorts agree very well. The previous studies pointed to sub-multiplicative response of the relative risk to joint action of radon and smoking with a reduction of the radon risk by some 20% (Leuraud et al. 2011; Luebeck et al. 1999). We observed a similar effect of on average 16% reduction for interaction between exposure to silica dust and radon.

The shape of the lag–response curves exhibits similar features. Estimates of peak risk between 10 and 15 year after exposure are broadly consistent. However, the lack of evidence of a risk more than 35 year after radon exposure in the Colorado cohort may be related to a small number of cases contributing for large time since exposure. In the Wismut cohort, the radon risk persists even after a time lag of 40 year, which is biologically more plausible.

The majority of uranium miner studies routinely rely on 5 year lags for cumulative exposure (see refs. (Schubauer-Berigan et al. 2009) for Colorado miners and (Kreuzer et al. 2018, 2015; Walsh et al. 2010) for Wismut miners). Yet, Fig. 3 shows that HRs from DLNMs at 5 year after exposure may have already reached half the maximum risk in some cases. Application of 5 year lags could underestimate the risk *shortly* after first exposure, but risks occurring much later than 5 year after exposure are still adequately described.

The non-linear exposure–response association to annual radon exposure rates exhibits break points between 20 WLM/yr (present study) and 50 WLM/yr (Gasparrini 2014) which mark a change to reduced slope (Fig. 3). The biological meaning of break points must not be over-interpreted, since they are intrinsic features in B-splines. A natural logarithm describes the exposure–response almost equally well (Aßenmacher 2016).

Comparison with standard radio-epidemiological and biologically based risk models

In Fig. 4, all three models predict a decreasing risk at old age but with markedly different trends. The ERR from the DLNM peaks at about 43 year as expected from the lag–response curves. The TSCE model does not exhibit a maximum risk, but the risk decays smoothly from a constant plateau. The course of the risk from the ERR model is dominated by an exponential decay at young ages, which is mitigated by a time-since-exposure effect at old ages. Whereas, for cumulative exposure, 100 WLM all models produce ERR estimates in the same range, for cumulative exposure 400 WLM, the ERR estimates of the DLNM are significantly lower consistent with results shown in Fig. 5.

While the ERR model includes the LNT assumption in its design, responses to the cumulative radon exposure in the TSCE model and the DLNM model can deviate from linearity if suggested by fits to the data. In DLNMs, the HR is roughly proportional to $\exp(\beta D)$, which, for small cumulative exposure, D is approximated by a linear response $1 + \beta D$. In Fig. 5, a low exposure rate of 12.5 WLM/yr leads to 150 WLM cumulative exposure at maximum. For cumulative exposure up to this, maximum linearity is supported by all three models. For higher cumulative exposure up to 1200 WLM, which is caused by an exposure rate of 100 WLM/yr, the response of the TSCE model shows a clear upward curvature, which is weakly reflected by the DLNM. This behavior is in line with findings for the Wismut cohort where non-linearity for ERR models has been tested by Walsh et al. (2010) (see the discussion of their Fig. 1). Statistical significance of a quadratic term for cumulative exposure disappeared after adjusting for exposure rate.

An analysis with descriptive Poisson regression models yielded a central estimate for ERR/100 WLM of 1.06 (95% CI 0.69; 1.42) (Walsh et al. 2010). The ERR was adjusted for EMs median age at exposure centered at 33 year, time since median exposure centered at 11 year, and exposure rate centered at 2.7 WL. Zaballa and Eidemüller (2016) reported a central estimate of 1.28 (95% CI 0.81; 1.77) from their ERR model using the same EMs time since median exposure and exposure rate. We find a corresponding estimate of 0.25 (95% CI 0.18; 0.31) for a rate of 32.4 WLM/yr (= 2.7 WL) and time since exposure between 9.5 and 12.5 year from our preferred DLNM. Our estimate is much lower than estimates from TSCE model and from the descriptive ERR model, which assumes a linear-quadratic attenuation effect for time since exposure in the exponent (Eq. 8).

Onset and duration of development for radon-related lung cancer

Drawing conclusions on lung cancer etiology from radio-epidemiological models, which merely rely on statistical associations, has strict limitations (Greenland 2017; Robins and Greenland 1989). As a necessary condition, the biological concept of cancer development must be specified (Beyea and Greenland 1999). For radiation-induced carcinogenesis, the biologically based TSCE model provides such a concept and has been successfully applied to a wide range of radio-epidemiological data sets (Rühm et al. 2017). By jointly analyzing results from DLNMs and TSCE models, we can gain some insight into the duration of development for radon-related lung cancer.

We interpret the latency period t_{lat} as the time span between the appearance of the first malignant cell to the time to death. This interpretation is commonly used in biologically based modeling of lung carcinogenesis (Geddes 1979; Luebeck et al. 1999; Zaballa and Eidemüller 2016). Latency t_{lat} is not yet accessible by direct measurement and depends strongly on model assumptions. In the present

study, the minimum lag (or intercept) l_0 is understood as the time period after which first exposure starts to increase the value for the hazard ratio above one. An estimate for the minimum lag l_0 can be gleaned from observational data with some uncertainty. For example, Heidenreich et al. (1999) estimated a minimum lag of 3 year after exposure for post-Chernobyl thyroid cancer incidence. According to the mechanistic model of carcinogenesis for miners, cohorts some time pass after first exposure to develop the first malignant cell (Luebeck et al. 1999; Zaballa and Eidemüller 2016). With these assumptions, minimum lag $l_0 >$ must always exceed (minimum) latency t_{lat}. However, as we argue below, both periods may be rather short.

Minimum lag for the onset of risk

Comprehensive investigations in the present study and in the Colorado study (Gasparrini 2014) suggest a minimum lag of 2 year for onset of the radiation risk. Although the study of Berhane et al. (2008) did not aim to determine the minimum lag period, their Fig. 3 supports a minimum lag of 2–3 year by extrapolation of the HR in the *low* exposure category.

It is instructive to apply findings from biologically based modeling of lung tumor growth for the assessment of results from the observational studies. In the analysis of Geddes (1979), minimal latencies were calculated under the assumption of an exponential tumor growth model, where growth starts with a single malignant cell. Exponential growth functions have been fitted to tumors with minimal diameter of 1 cm, corresponding to about 10^9 cells. A tumor eventually becomes fatal with a size of 10 cm or 10^{12} cells (Geddes 1979, Table I). Below size 1 cm, growth dynamics is inferred by extrapolation and may not necessarily be correct, because cancer stem cells develop from small precursor lesions which do not exhibit the molecular spectrum of a full blown tumor. For lung adenocarcinoma, atypical adenomatous hyperplasia (AAH) are considered as putative precursor lesions (Pan et al. 2018). Often AAH are converted to malignancy by a second mutation in a tumor suppressor gene, i.e., TP53. In fact, mechanistic models of carcinogenesis for miners cohorts are based on this assumption (Luebeck et al. 1999; Zaballa and Eidemüller 2016). AAH are about 5 mm large, when they possibly become malignant. A back-of-the-envelope calculation suggests that an AAH would turn into a fatal tumor after about 13 doublings. Based on the doubling times of Geddes (1979) (Table II), short latency periods would be conceivable, in particular, if the carcinogenic effect of radon exposure targets advanced precursor lesions as in the mechanistic miners models. Applying the lowest estimate for a doubling time of 29 d pertaining to small (oat) cell carcinoma results in a latency period of about 1 year well below the minimum lag of 2 year. As an implication, the minimum period for the appearance of a second (or transforming) oncogenic mutation after first exposure would be also 1 year.

Hence, simple consideration of tumor growth dynamics confers biological plausibility to a minimal lag time of about 2 year, which has been found in observational studies.

Duration of development for radon-related lung cancer

Analysis of both experimental animal data and miner cohorts with mechanistic TSCE models consistently revealed as the main radon target clonal growth, which is enhanced by reduced inactivation of initiated cells (Eidemüller et al. 2012; Heidenreich et al. 1999; Kaiser et al. 2004; Luebeck et al. 1999; Zaballa and Eidemüller 2016). The growth curves are characterized by linear increase at low exposure rates which are followed by leveling at high exposure rates. Radiation-induced inflammation has been found to increase clonal expansion in animal studies (Harding et al. 2017). Thus, it is plausible to propose inflammation of the lung epithelium as the underlying mechanism for non-linear behavior of clonal growth (Zaballa and Eidemüller 2016).

Luebeck et al. (1999) estimated a mean latency period of 9 year from the appearance of the first cancer cell to lung cancer death for all histologic lung cancer types combined. Geddes (1979) Table IV reports a mean latency of 11 years similar to ref. (Luebeck et al. 1999). Results of the present study suggest that onset of radon-induced lung inflammation shapes the exposure–response curves of DLNMs starting about 2 year after first exposure with a mean lag of 15 year. Comparing the estimates for mean lag and mean latency, we speculate that malignant cells carrying a second oncogenic mutation appear on average about 5 years after the first exposure.

Limitations

Since the present study is mainly concerned with radon risk, the influence of other confounders has not been given the same attention. In particular, we did not fully characterize the exposure–lag–response surface for silica dust exposure. However, we estimate a reduction of the radiation risk of 16% on average. Smoking information is available for 56% of Wismut miners hired after 1960 (Kreuzer et al. 2018). However, these miners were mainly exposed at low exposure rates, which do not produce a pronounced exposure–lag–response. The ERR/WLM was by a factor of 1.7 higher for non/light smokers compared to moderate/heavy smokers. Correction for smoking in case–control studies of European miners cohorts resulted in a moderate reduction of ERR estimates by some 20% (Leuraud et al. 2011).

The impact of exposure uncertainties on risk estimates has not yet been evaluated for the Wismut cohort, but studies

for the cohort of French miners suggest only minor corrections (Hoffmann et al. 2017).

Based on information criteria for goodness-if-fit, comparison of DLNMs with ERR and TSCE models of ref. (Zaballa and Eidemüller 2016) was not possible. A comparison of absolute values for the AIC and BIC from Cox regression with those from individual likelihood regression used in ref. (Zaballa and Eidemüller 2016) is not straightforward even for identical data sets. In further studies, the DLNM framework needs to include Poisson regression and individual likelihood regression, which are methods of choice in radiation epidemiology.

For pertinent exposure scenarios, a maximum time lag of 40 year is too short for the Wismut cohort where miners have been followed up until 57 year after the first exposure. The maximum lag was chosen to facilitate a direct comparison with the result for the Colorado cohort from Gasparrini (2014) and should be relieved in future studies.

Information of lung cancer histology is only available for a fraction of Wismut patients. From a case-based analysis, (Kreuzer et al. 2000) conclude that all cell types were associated with radon exposure, but high radon exposure tended to increase the proportion of small cell carcinoma and squamous cell carcinoma at the expense of adenocarcinoma. A recent study on Ontario miners reported highly significant radon-related ERR estimates for small cell carcinoma and squamous cell carcinoma, and for adenocarcinoma, the risk was marginally significant (Ramkissoon et al. 2018). In Japanese, a-bomb survivors the predominant histologic types exhibit differential radiation risk for a mixed field of photons and neutrons (Egawa et al. 2012). However, for relative risk estimates, the trend was reversed. Adenocarcinoma revealed a stronger dose response than squamous cell carcinoma and small cell carcinoma.

Conclusion

As a boost for its validity, the DLNM approach yielded compatible exposure–lag–response models for miners cohorts of the German Wismut company and the Colorado Plateau in the United States. In both cohorts, our data-driven approach supported an estimate of about 2 year for the minimum lag for the onset of radiation risk. These findings are biologically plausible and compatible with results of a tumor growth model. However, uncertainties for the estimate could not be quantified, but might be large due to a lack of direct measurements. Furthermore, we believe that the common assumption of a 5 year minimal lag for response to radon exposure does not influence risk estimates in miner studies unless the early onset of risk is the special focus.

After comparing exposure–responses for biological processes in mechanistic risk models with exposure–responses for hazard ratios in DLNMs, we surmise a mean period of 15 year for radiation-induced lung carcinogenesis in radon-exposed uranium miners. The period probably covers the onset of radiation-induced inflammation until cancer death.

To conclude, application of the DLNM framework in radiation epidemiology provides new insight into age-risk patterns and cancer etiology, which is complementary to results gained from both the standard descriptive approach and biologically based modeling. We recommend to add it to the radio-epidemiological toolbox for future investigations.

Acknowledgements Dr. Gasparrini was supported by the Medical Research Council UK (Grant IDs: MR/M022625/1 and MR/R013349/1). The authors would like to thank Dr. Kreuzer and Dr. Sobotzki (Federal Office for Radiation Protection) for the excellent cooperation in providing the data and for their comments. We also thank two anonymous referees for their helpful comments.

Compliance with ethical standards

Conflict of interest The authors declare no conflicts of interests.

Appendix

Results of DLM analysis

For all models, the maximum time lag L was fixed to 40 year as in Gasparrini (2014). Each model is adjusted for age at begin of employment (*abe*) and the calendar year (*cal*) (Eq. (1)).

Models L1 and L3 apply constant and piecewise constant functions for $w_x(\ell)$, respectively. Piecewise constant functions possess three cut-off points at time since exposure 10 year, 20 year, and 30 year (See Tables 2, 3).

Models L2 and L4 correspond to models L1 and L3 albeit with additional adjustment for silica dust. The corresponding exposure–response $f(z_{t-\ell})$ is specified as a linear threshold function. Response to silica exposure is restrained to zero below a threshold of 0.92 mg/m^3/yr; above threshold $f(z_{t-\ell})$ increases linearly. The threshold value is motivated in ref. (Zaballa and Eidemüller 2016) as break point for the capability of silica dust removal. The lag–response $w_z(\ell)$ for silica dust is defined as a piecewise constant function with two cut-off points at equally spaced quantiles of the distribution of the lags. There is no evidence of departure from of multiplicative joint effect for exposure to radon and silica dust. This choice yields an acceptable flexibility under the condition of not spending too many model parameters *df* on a complicated modeling of silica dust. In this way, all models of the present study consume five parameters *df* on controlling for the confounders of silica dust, age at begin of employment, and the calendar year (Figs. 6, 7, 8, 9, 10, 11).

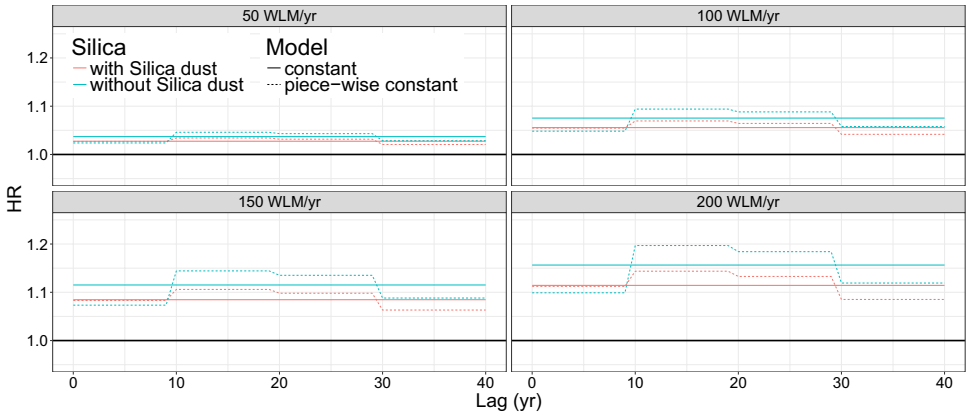

Fig. 6 Comparison of lag–response curves for the hazard ratio (HR) of DLMs L1–L4 for four different radon exposure rates 50 WLM/yr, 100 WLM/yr, 150 WLM/yr, and 200 WLM/yr, in models L2 and L4 (red lines) silica dust is a confounder but not in models L1 and L3 (blue lines); for models L1 and L2 (solid lines), the lag–response is constant; for models L3 and L4 (dashed lines), the lag–response is piecewise constant with cut-off points at 10 year, 20 year, and 30 year

Table 2 Properties and goodness-of-fit for DLMs L1–L5 with a linear exposure–response $f(x_{t-\ell})$ to annual radon exposure rates and varying shapes of lag–responses $w_x(\ell)$; for piecewise constant, lag–response cut-offs are located 10 year, 20 year, and 30 year; *df* denotes the number of model parameters, lowest values for AIC and BIC in bold; L5 is the preferred DLM

Model	$w_x(\ell)$	AIC	BIC	*df*	silica dust	*p*
L1	Constant	58427.86	58445.87	3	No	–
L2	Constant	58353.14	**58389.17**	6	Yes	< 0.01
L3	Piecewise constant	58404.23	58440.26	6	No	< 0.01
L4	Piecewise constant	58350.07	58404.11	9	Yes	0.028
L5	B-Spline (degree 2, 1 knot)[a]	**58345.58**	58393.62	8	Yes	–

The last column contains the *p* values of LRTs where L2 and L3 are tested against L1 and L4 is tested against L2. All p values are smaller than 0.05 which indicates a superior goodness-of-fit for more complex models and models controlling for silica dust. Model L5 cannot be tested via LRT as it is not nested. a minimum lag ℓ_0 set to 2 year

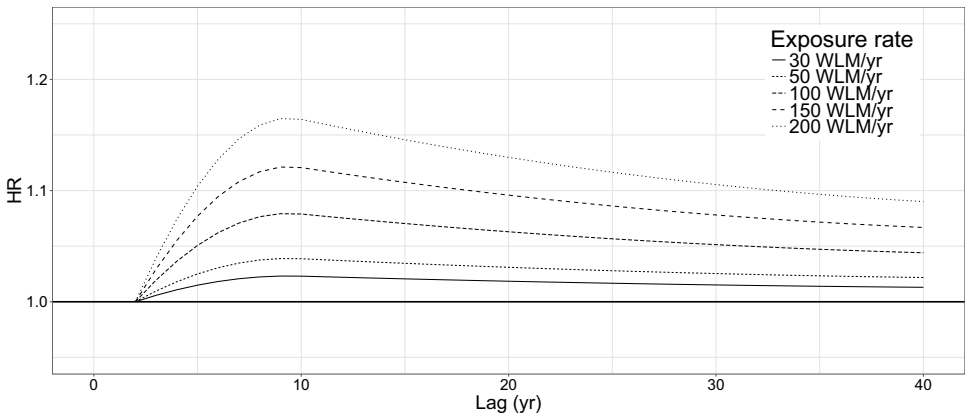

Fig. 7 Lag–response curves for the hazard ratio (HR) of the preferred DLM L5 for five radon exposure rates between 30 WLM/yr and 200 WLM/yr

Comparing models with adjustment for silica dust L2 and L4 with their counterparts L1 and L3 without adjustment reveals improvement in the AIC of at least 50 points and likewise improvements in the BIC (Table 2). These findings justify the inclusion of silica dust adjustment in the main analysis of the present study. Figure 6 depicts lag–responses

for models L1–L4 with more pronounced shapes for increasing radon exposure rates. In terms of goodness-of-fit, the introduction of more complex shapes for the lag–response yields moderate improvements (Table 2).

The next phase of model development was concerned with improvements of the lag–response $w_x(\ell)$ of DLMs. To determine the shape of $w_x(\ell)$, we tested models with B-Splines of degrees one to six with zero up to five knots on equally spaced quantiles of the weighted lag distribution. The intercept of the hazard ratio (HR) on the y axis was determined in the fits. For most of the curves, the intercepting HR was estimated < 1, and the HR exceeded 1 only after a lag of 3 years. This observation strengthens the argument that no risk occurs in the early years after exposure. In our models, we set the minimum lag to 2 year. However, we do not allow hormetic effects in the lag–response and fix HRs smaller than one at early lags to zero. For the preferred DLM L5, the shape of the lag–response is shown in Fig. 7 for various radon exposure rates. Modeled with a quadratic B-spline and one knot, lag–response curves for model L5 exhibit a maximum at about 9 year after first exposure followed by a steady decline. Properties of model L5 are given in Table 2.

DLNM NL3 with right-constrained lag–response at 40 year

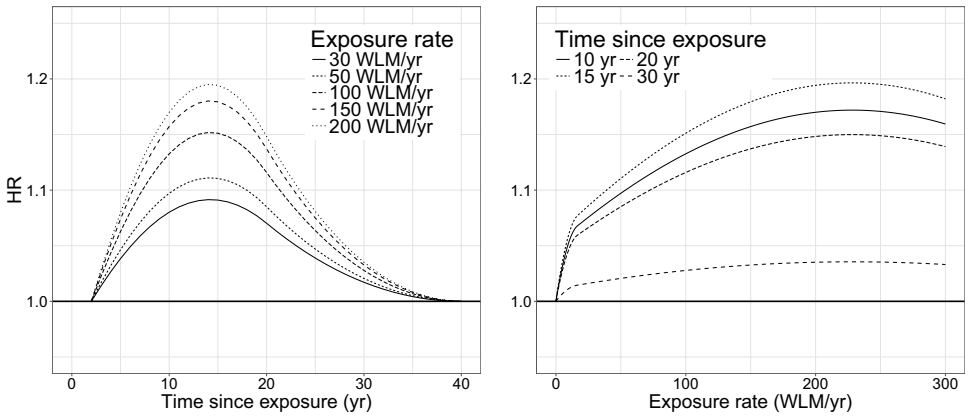

Fig. 8 Selected lag–response curves of the hazard ratio (HR) for exposure rates between 30 and 200 WLM/yr (left panel) and exposure–response curves for time since exposure between 10 and 30 year (right panel) for DLNM NL3 with right-constrained lag–response function at 40 year

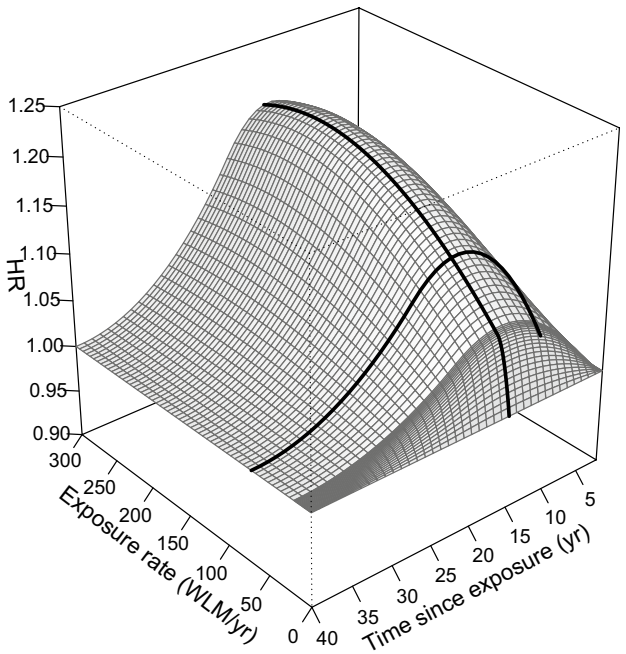

Fig. 9 The exposure–lag–response surface for the hazard ratio (HR) of DLNM NL3 with right-constrained lag–response function at 40 year

Estimates for confounders age at begin of employment, calendar year, and silica dust exposure for the preferred DLNM NL4

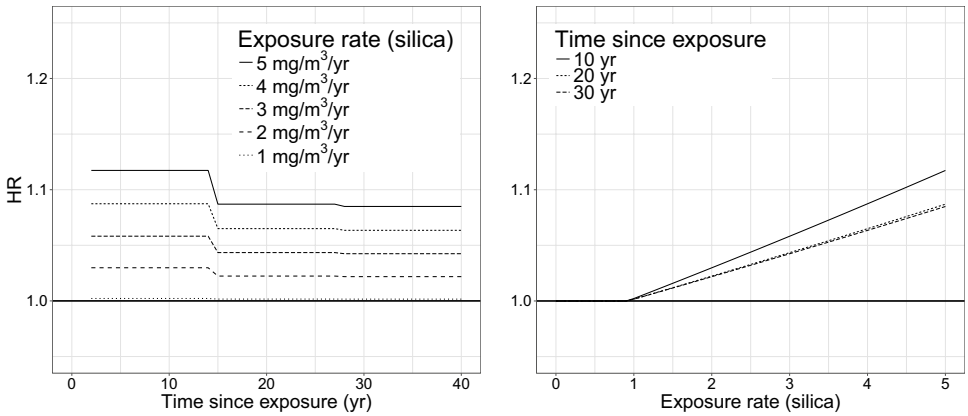

Fig. 10 Selected lag–response curves of the hazard ratio (HR) for exposure rates between 1 and 5 $\frac{\mathrm{mg/m^3}}{\mathrm{yr}}$ (left panel) and exposure–response curves for time since exposure between 10 and 30 year (right panel) for silica dust for the preferred DLNM NL4

Table 3 Estimates of *cal* and *abe* from DLNM NL4

	β	$exp(\beta)$	σ_β	p value
cal	− 0.0101	0.9900	0.0044	0.0233
abe	− 0.0231	0.9772	0.0048	0.0000

Table 4 Estimates of cross-basis coefficients for the preferred DLNM NL4

	$\boldsymbol{\eta}_{x,[i,j]}$	$\exp(\boldsymbol{\eta}_{x,[i,j]})$	$\sigma_{\boldsymbol{\eta}_{x,[i,j]}}$	p value
$B1_{\mathrm{Exp}} \cdot B1_{\mathrm{lag}}$	− 0.0587	0.9430	0.0184	0.0014
$B1_{\mathrm{Exp}} \cdot B2_{\mathrm{lag}}$	0.0835	1.0871	0.0250	0.0008
$B1_{\mathrm{Exp}} \cdot B3_{\mathrm{lag}}$	− 0.1075	0.8980	0.0381	0.0047
$B2_{\mathrm{Exp}} \cdot B1_{\mathrm{lag}}$	0.0691	1.0715	0.0241	0.0041
$B2_{\mathrm{Exp}} \cdot B2_{\mathrm{lag}}$	0.0456	1.0466	0.0241	0.0590
$B2_{\mathrm{Exp}} \cdot B3_{\mathrm{lag}}$	0.0176	1.0177	0.0251	0.4841
$B3_{\mathrm{Exp}} \cdot B1_{\mathrm{lag}}$	0.3600	1.4333	0.0988	0.0003
$B3_{\mathrm{Exp}} \cdot B2_{\mathrm{lag}}$	0.0698	1.0723	0.0824	0.3970
$B3_{\mathrm{Exp}} \cdot B3_{\mathrm{lag}}$	0.0997	1.1048	0.0756	0.1875
$B4_{\mathrm{Exp}} \cdot B1_{\mathrm{lag}}$	0.1133	1.1199	0.1128	0.3154
$B4_{\mathrm{Exp}} \cdot B2_{\mathrm{lag}}$	0.0901	1.0942	0.1022	0.3784
$B4_{\mathrm{Exp}} \cdot B3_{\mathrm{lag}}$	0.0718	1.0744	0.1001	0.4731

Baseline rates λ_0 of lung cancer mortality from the preferred DLNM NL4

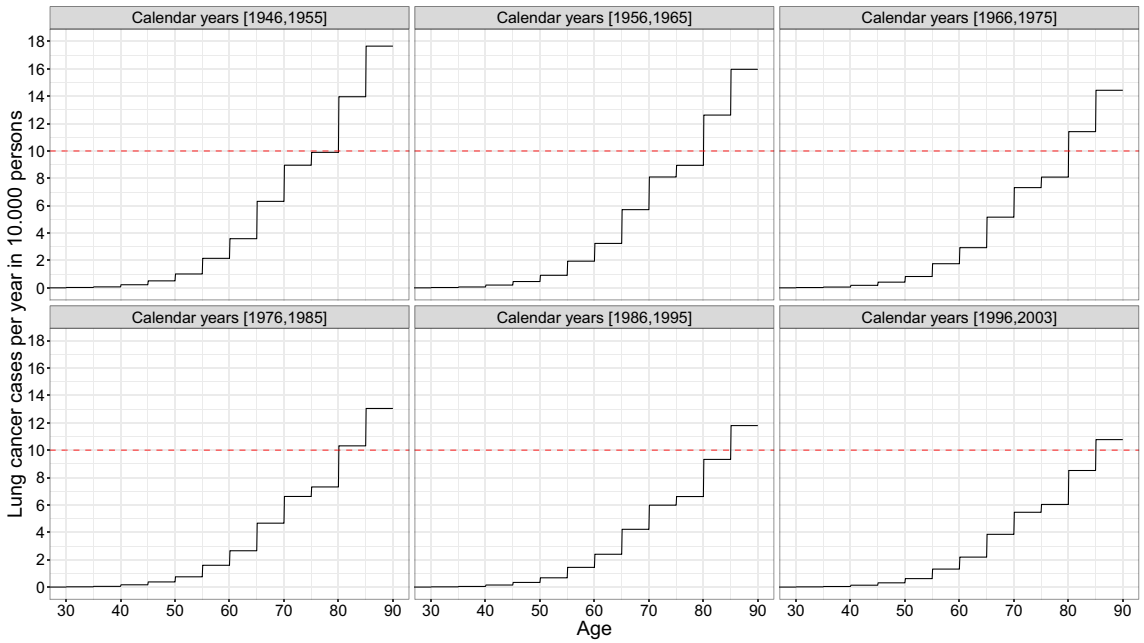

Fig. 11 Baseline rates of lung cancer mortality from the preferred DLNM NL4 are averaged among age groups of 5 years and calculated separately for six calendar periods between 1946 and 2003

References

Alberg AJ, Brock MV, Ford JG, Samet JM, Spivack SD (2013) Epidemiology of lung cancer. Chest 143(5):e1S–e29S

Armstrong B (2006) Models for the relationship between ambient temperature and daily mortality. Epidemiology 17(6):624–631

Aßenmacher M (2016) The exposure–lag–response association between occupational radon exposure and lung cancer mortality. Master's thesis, LMU Munich, Department of Statistics, Ludwigstr. 33, 80539 Munich. https://epub.ub.uni-muenchen.de/39110/

BEIR VI: Health Effects of Exposure to Radon. National Academy Press, Washington, D. C. (1999). National Research Council, Committee on Health Risks of Exposure to Radon

Bender A, Scheipl F, Hartl W, Day AG, Küchenhoff H (2018) Penalized estimation of complex, non-linear exposure–lag–response associations. Biostatistics 20(2):315–331

Berhane K, Hauptmann M, Langholz B (2008) Using tensor product splines in modeling exposure-time-response relationships: application to the Colorado plateau uranium miners cohort. Stat Med 27(26):5484–96. https://doi.org/10.1002/sim.3354

Beyea J, Greenland S (1999) The importance of specifying the underlying biologic model in estimating the probability of causation. Health Phys 76(3):269–274

Cox DR (1975) Partial likelihood. Biometrika 62(2):269–276

Efron B (1977) The efficiency of Cox's likelihood function for censored data. J Am Stat Assoc 72(359):557–565

Egawa H, Furukawa K, Preston D, Funamoto S, Yonehara S, Matsuo T, Tokuoka S, Suyama A, Ozasa K, Kodama K et al (2012) Radiation and smoking effects on lung cancer incidence by histological types among atomic bomb survivors. Radiat Res 178(3):191–201

Eidemüller M, Jacob P, Lane RS, Frost SE, Zablotska LB (2012) Lung cancer mortality (1950–1999) among Eldorado uranium workers: a comparison of models of carcinogenesis and empirical excess risk models. PloS one 7(8):e41431

Gasparrini A (2011) Distributed lag linear and non-linear models in R: the package dlnm. J Stat Softw 43(8):1–20

Gasparrini A (2014) Modeling exposure-lag-response associations with distributed lag non-linear models. Stat Med 33(5):881–99. https://doi.org/10.1002/sim.5963

Gasparrini A, Armstrong B, Kenward MG (2010) Distributed lag non-linear models. Stat Med 29(21):2224–34. https://doi.org/10.1002/sim.3940

Gasparrini A, Scheipl F, Armstrong B, Kenward MG (2017) A penalized framework for distributed lag non-linear models. Biometrics 73(3):938–948

Geddes DM (1979) The natural history of lung cancer: a review based on rates of tumour growth. Br J Dis Chest 73(1):1–17

Fitzmaurice C, Allen C, Barber RM, Barregard L, Bhutta ZA, Brenner H, Fleming T (2017) Global Burden of disease cancer collaboration: global, regional, and national cancer incidence, mortality, years of life lost, years lived with disability, and disability-adjusted life-years for 32 cancer groups, 1990 to 2015: A systematic analysis for the global burden of disease study. JAMA Oncol 3(4):524–548. https://doi.org/10.1001/jamaoncol.2016.5688

Greenland S (2017) For and against methodologies: some perspectives on recent causal and statistical inference debates. Eur J Epidemiol 32(1):3–20. https://doi.org/10.1007/s10654-017-0230-6

Harding SM, Benci JL, Irianto J, Discher DE, Minn AJ, Greenberg RA (2017) Mitotic progression following DNA damage enables pattern recognition within micronuclei. Nature 548(7668):466–470. https://doi.org/10.1038/nature23470

Hauptmann M, Berhane K, Langholz B, Lubin J (2001) Using splines to analyse latency in the colorado plateau uranium miners cohort. J Epidemiol Biostat 6(6):417–424

Heidenreich WF, Jacob P, Paretzke HG, Cross FT, Dagle GE (1999) Two-step model for the risk of fatal and incidental lung tumors in rats exposed to radon. Radiat Res 151(2):209–17

Heidenreich WF, Kenigsberg J, Jacob P, Buglova E, Goulko G, Paretzke HG, Demidchik EP, Golovneva A (1999) Time trends of thyroid cancer incidence in Belarus after the Chernobyl accident. Radiat Res 151(5):617–25

Hoffmann S, Rage E, Laurier D, Laroche P, Guihenneuc C, Ancelet S (2017) Accounting for Berkson and classical measurement error in radon exposure using a Bayesian structural approach in the analysis of lung cancer mortality in the French cohort of uranium miners. Radiat Res 187(2):196–209. https://doi.org/10.1667/RR14467.1

Kaiser JC, Heidenreich WF, Monchaux G, Morlier JP, Collier CG (2004) Lung tumour risk in radon-exposed rats from different experiments: comparative analysis with biologically based models. Radiat Environ Biophys 43(3):189–201. https://doi.org/10.1007/s00411-004-0251-x

Kreuzer M, Fenske N, Schnelzer M, Walsh L (2015) Lung cancer risk at low radon exposure rates in German uranium miners. Br J Cancer 113(9):1367–1369

Kreuzer M, Müller KM, Brachner A, Gerken M, Grosche B, Wiethege T, Wichmann HE (2000) Histopathologic findings of lung carcinoma in German uranium miners. Cancer 89(12):2613–21

Kreuzer M, Schnelzer M, Tschense A, Walsh L, Grosche B (2010) Cohort profile: the German uranium miners cohort study (WISMUT cohort), 1946–2003. Int J Epidemiol 39(4):980–7. https://doi.org/10.1093/ije/dyp216

Kreuzer M, Sobotzki C, Schnelzer M, Fenske N (2018) Factors modifying the radon-related lung cancer risk at low exposures and exposure rates among German uranium miners. Radiat Res 189(2):165–176. https://doi.org/10.1667/RR14889.1

Küchenhoff H, Deffner V, Aßenmacher M, Neppl H, Kaiser C, Güthlin D et al (2018) Ermittlung der Unsicherheiten der Strahlenexpositionsabschätzung in der Wismut-Kohorte – Teil I – Vorhaben 3616s12223. Bundesamt für Strahlenschutz (BfS)

Lehmann F (2004) Job-exposure-matrix Ionisierende Strahlung im Uranerzbergbau der ehemaligen DDR (Version 06/2003). Bergbau BG, Gera

Lehmann F, Hambeck L, Linkert K, Lutze H, Meyer H, Reiber H, Renner H, Reinisch A, Seifert T, Wolf F (1998) Belastung durch ionisierende Strahlung im Uranerzbergbau der ehemaligen DDR. Hauptverband der gewerblichen Berufsgenossenschaften, St. Augustin

Leuraud K, Schnelzer M, Tomasek L, Hunter N, Timarche M, Grosche B, Kreuzer M, Laurier D (2011) Radon, smoking and lung cancer risk: results of a joint analysis of three european case-control studies among uranium miners. Radiat Res 176(3):375–87

Luebeck EG, Heidenreich WF, Hazelton WD, Paretzke HG, Moolgavkar SH (1999) Biologically based analysis of the data for the Colorado uranium miners cohort: age, dose and dose-rate effects. Radiat Res 152(4):339–351

NRC: Health risks from exposure to low levels of ionizing radiation: BEIR VII - phase 2. United States National Academy of Sciences, National Academy Press, Washington, D. C. (2006). United States National Research Council, Committee to assess health risks from exposure to low levels of ionizing radiation

Pan X, Yang X, Li J, Dong X, He J, Guan Y (2018) Is a 5-mm diameter an appropriate cut-off value for the diagnosis of atypical adenomatous hyperplasia and adenocarcinoma in situ on chest computed tomography and pathological examination? J Thorac Dis 10(Suppl 7):S790–S796. https://doi.org/10.21037/jtd.2017.12.124

R Core Team (2019) R: a language and environment for statistical computing. R Foundation for Statistical Computing, Vienna, Austria. https://www.R-project.org/. Accessed 11 Mar 2019

Ramkissoon A, Navaranjan G, Berriault C, Villeneuve PJ, Demers PA, Do MT (2018) Histopathologic analysis of lung cancer incidence associated with radon exposure among ontario uranium miners. Int J Environ Res Public Health 15(11):2413. https://doi.org/10.3390/ijerph15112413

Richardson D, Sugiyama H, Nishi N, Sakata R, Shimizu Y, Grant EJ, Soda M, Hsu WL, Suyama A, Kodama K, Kasagi F (2009) Ionizing radiation and leukemia mortality among Japanese atomic bomb survivors, 1950–2000. Radiat Res 172(3):368–82. https://doi.org/10.1667/RR1801.1

Robins JM, Greenland S (1989) Estimability and estimation of excess and etiologic fractions. Stat Med 8(7):845–859

RStudio Team (2015) RStudio: integrated development environment for R. RStudio, Inc., Boston, MA. http://www.rstudio.com/. Accessed 11 Mar 2019

Rühm W, Eidemüller M, Kaiser JC (2017) Biologically-based mechanistic models of radiation-related carcinogenesis applied to epidemiological data. Int J Radiat Biol 93(10):1093–1117

Schubauer-Berigan MK, Daniels RD, Pinkerton LE (2009) Radon exposure and mortality among white and American Indian uranium miners: an update of the Colorado plateau cohort. Am J Epidemiol 169(6):718–730

Therneau TM (2015) A Package for Survival Analysis in S http://CRAN.R-project.org/package=survival. Version 2.38-3

Therneau TM, Grambsch PM (2000) Modeling survival data: extending the Cox model. Springer, New York

UNSCEAR (2009) 2006 REPORT, vol. I, Effects of Ionizing Radiation, Report to the General Assembly Annex E: Sources-to-Effects Assessment for Radon in Homes and Workplaces. United Nations, New York

Valentin J (ed) (2007) The 2007 Recommendations of the International Commission on Radiological Protection. Annals of the ICRP. Elsevier, Amsterdam (**Publication 103**)

Walsh L, Dufey F, Tschense A, Schnelzer M, Grosche B, Kreuzer M (2010) Radon and the risk of cancer mortality-internal Poisson models for the German uranium miners cohort. Health Phys 99(3):292–300. https://doi.org/10.1097/HP.0b013e3181cd669d

Walsh L, Grosche B, Schnelzer M, Tschense A, Sogl M, Kreuzer M (2015) A review of the results from the German Wismut uranium miners cohort. Radiat Prot Dosimetry 164(1–2):147–53. https://doi.org/10.1093/rpd/ncu281

Walsh L, Tschense A, Schnelzer M, Dufey F, Grosche B, Kreuzer M (2010) The influence of radon exposures on lung cancer mortality in German uranium miners, 1946–2003. Radiat Res 173(1):79–90. https://doi.org/10.1667/RR1803.1

Wickham H (2016) ggplot2: elegant graphics for data analysis. Springer, New York

Zaballa I, Eidemüller M (2016) Mechanistic study on lung cancer mortality after radon exposure in the Wismut cohort supports important role of clonal expansion in lung carcinogenesis. Radiat Environ Biophys 55(3):299–315